Journal of Magnetism and Magnetic Materials 484 (2019) 350–355

Contents lists available at ScienceDirect

Journal of Magnetism and Magnetic Materials

journal homepage: www.elsevier.com/locate/jmmm

Research articles

Microstructure and magnetic properties of dilute nanocrystalline Fe-Si prepared by high energy ball milling

Trevor Clark, Suveen Nigel Mathaudhu*

Materials Science and Engineering, University of California, Riverside, United States

ARTICLE INFO

Keywords:
High energy ball milling
Mechanical alloying
Nanocyrstalline
Soft magnetic

ABSTRACT

The microstructure and magnetic properties of nanocrystalline Fe-Si soft magnetic material fabricated by high energy vibratory milling are investigated. Fe-Si × wt% (x = 1.78, 3.51, 3.80, 5.08, 6.06, 6.98, 8.04) compositions are studied, with the 3.5 wt% case being used as a model system to investigate effects of processing time. X-ray diffraction (XRD) measurements indicate that the Si is fully in solution in the Fe lattice and no ordered phases are present. It is shown that microstructural evolution is accelerated compared with previously observed lower energy milling processes of iron-based alloys. It is also shown that magnetic properties are in disagreement with the formulas derived from the random anisotropy model, and explanations are provided for potential sources of this discrepancy in this and other reported work.

1. Introduction

Magnetic materials are critical in carbon neutral technologies such as clean energy production in the form of hydroelectric, and wind power generation. With the rising cost of critical rare earth permanent magnet materials, it is becoming more important to improve the performance and efficiency of rare earth free magnetic devices. Of immediate interest is the issue of core loss, which is an important metric in determining the efficiency of electric motors and generators.

Soft magnetic materials are characterized by their low coercivity and high magnetic permeability [1], and in these materials, hysteresis loss can be the largest source of core loss in a device. Some of the most common soft magnet materials are Fe-Si alloys, which are widely used as magnetic cores in electrical applications such as transformers and electric motors because of their excellent soft magnetic properties [2–4]. The addition of Si into Fe not only results in a reduced magnetic anisotropy and coercive force, but also increases electrical resistivity, and therefore reduces eddy current loss [5]. However, Fe-Si alloys containing more than 6.5 wt% silicon are brittle and difficult to cold-roll and therefore are near impossible to obtain by conventional melting and casting production methods. When traditionally casting these high silicon alloys, two ordered phases are present: B2 and DO_3 [6]. These ordered phases cause embrittlement by hindering of dislocation movement, and they also reduce the magnetic performance due to the ordered positions of the Si in the lattice [7,8].

It has been reported that by engineering the grain size to the nanocrystalline regime, the hysteresis loss can be reduced through lowering of the coercivity [9,10]. Nanostructured or nanocrystalline materials have different physical properties than non-crystalline, single-crystalline, and oligocrystalline materials, such as increased strength, hardness, and control of magnetic coercivity [9,11]. The unique properties of nanocrystalline soft magnets occur when the crystallite size is less than the ferromagnetic correlation length (typically 20–40 nm) [12]. This allows the magnetic coupling of neighboring crystallites and produces an averaging effect of local magnetic anisotropies leading to a significant reduction in magnetic anisotropy. These nanocrystalline Fe-Si alloys often exhibit considerably improved properties, including mechanical properties, electrical resistivity, thermal conductivity, and soft magnetic properties over coarse-grained polycrystalline materials [9,13]. One way of achieving such nanostructures is through mechanical alloying (MA), which consists of elemental or pre-alloyed powder particles milled with media (usually stainless steel balls). These particles undergo severe deformation and have stored energy in excess of that in an equilibrium/stable structure [14,15]. This excess energy can allow for enhanced solubility of Si in Fe, and favors the preferred disordered crystal structure over the detrimental brittle ordered phases [16,17]. Higher energy mills such as shaker or vibratory mills have a high frequency of highly mechanical frontal impacts compared to lower energy planetary mills that have much lower frequency of impacts and higher fraction of tangential collisions that produce more heat [14,15]. The high energy ball mills can allow for more stored energy resulting in and quicker processing times [18]. This has been shown to be a scalable

* Corresponding author.
E-mail address: smathaudhu@engr.ucr.edu (S.N. Mathaudhu).

https://doi.org/10.1016/j.jmmm.2019.03.070
Received 22 February 2019; Accepted 14 March 2019
Available online 15 March 2019
0304-8853/

way of producing nanostructured, supersaturated fully-alloyed powders [15,19–23]. For the Fe-Si system, literature has reported on the planetary milling and its ability to make supersaturated solid solutions [20,21,23].

In this work, we aim to synthesize a range of Fe-Si alloys using mechanical alloying to obtain a high Si concentration and small grain size, and to explore the role of process parameters on the resulting microstructure and magnetic properties. In order to explore the role of processing parameters, the Fe 3.5wt% Si alloy is used as a model system. Unlike prior studies which have utilized lower-energy ball milling [16,20–24], this work will implement high energy shaker mills and analyzes both the effect of time and alloy content on magnetic and structural properties. More specifically, the effects of milling time and Si concentration on the morphological, structural, and magnetic properties of the powder are presented and discussed.

2. Materials and methods

In this experiment, iron powder (325 mesh, 99.8 wt% purity) and silicon powder (325 mesh 99.0 wt% purity) (Atlantic Equipment Engineers) were mechanically alloyed. Powders were mixed in compositions of Fe-Si × wt% (x = 1.78, 3.51, 3.80, 5.08, 6.06, 6.98, 8.04) with the 3.5 wt% case being used as a model system to investigate effects of processing time. Milling loads were 5.0 g of powder and 50 g of ¼ inch 440C stainless steel balls packed into a 65 mL 440C stainless steel vial under argon atmosphere. No process control agent was used. Powder was milled in a SPEX 8000D high energy shaker mill for 5, 10 15, and 20 h with a duty cycle of 15 min on and 5 min off to prevent excess heat buildup. The inner surface of the milling vial and the balls were pre-coated with elemental iron beforehand in an attempt to limit contamination from chromium in the stainless steel.

To determine crystallite size, lattice strain, and lattice parameter, powder specimens were analyzed by a Rigaku Miniflex 600 X-ray diffractometer (XRD) on an air sensitive holder with zero background substrate using Cu Kα (λ = 0.15405 nm) radiation from 36° to 120° 2θ. The Williamson-Hall method was used to estimate crystallite size and lattice spacing. Magnetic coercivity, saturation, and hysteresis were measured with a MicroSense vibrating sample magnetometer (VSM) with maximum magnetic field of 2.3 T. Microstructure and powder morphology were investigated using a FEI NovaNano 450 scanning electron microscope (SEM).

3. Results and discussion

3.1. Morphology

During mechanical alloying, powder particles undergo severe mechanical deformation and are repeatedly deformed, cold welded, fractured and rewelded [15]. Fig. 1 shows SEM micrographs of the starting (Fig. 1a and b) iron and silicon powders respectively. The iron powder was produced by gas atomization and has a characteristic pitted and rounded surface. The silicon powder has a mixture of larger faceted particles and smaller particles. The effect of milling time on the alloyed powder morphology was investigated on Fe 3.5 wt% Si, and it is observed that after mechanical alloying (Fig. 1c) the powder is more uniform in shape and size. The mechanically alloyed powder surface shows characteristic signs of cold welding and fracture sites. The brittle Si powder fractures much more than the comparatively soft Fe, with the Si then diffusing into the lamella structures of the metal powder. These lamella-like structures are shown in Fig. 2, and are characteristic of cold welding, with the large cracks showing fracture. Longer milling times were observed to produce a more uniform size distribution of particles (Fig. 3).

3.2. Structural properties

X-ray diffraction patterns (Fig. 4.) of the powders at various stages of milling show BCC Fe peaks, and no presence of Si peaks after 5 h of milling and on. This indicates that the Si may have dissolved into the BCC Fe solution and a solid solution of BCC-Fe(Si) has formed. Peaks are broad and have diminished intensity and peak width and intensity appears constant after 5 h of milling. There is no presence of the superlattice peaks of D03 phase indicating that no ordering of the Si is occurring. The crystallite size also appears to be constant after 5 h of milling (Fig. 5). This is a relatively short time to steady-state compared to literature which reports times of 40 h and 24 h [20,24,25]. More collisions and a higher differential velocity in collisions seen in shaker mills may increase the rate of cold welding and fracture events leading to a reduced time to steady state [14,15,18]. More specifically, the powders may be reaching a steady-state after this shorter milling time because of the increased energy of the shaker mill as compared to the planetary ball mills and attritor mills used in other studies [18,20,23,24,26]. Perez et al. show that for the FeBSi system mechanically alloyed by SPEX mill, the grain size reduces to 90 nm after only 0.5 h of milling and reaches minimum grain size of 12 nm after 4–8 h [17].

A range of alloys with different Si concentration were prepared the same via mechanical alloying process, and 5 h of milling. Fig. 6 shows the x-ray diffraction spectra. Each spectrum lacks the peaks for Si, indicating that the Si is likely in BCC-Fe solution. The lattice parameter (Fig. 7) shows a general decrease in spacing with increasing Si content. Si has a similar, but slightly smaller radius to Fe, and substitutes Fe to occupy the same lattice sites, and this could be responsible for the decreased lattice parameter [7]. The crystallite size appears be minimally, affected, if at all, within the reported range of Si content (Fig. 7). Bahrami and colleagues have also shown that crystallite size, calculated by Williamson-Hall method to be approximately 20 nm, is constant with Si content in Permalloy over 5 at% after planetary milling has reached steady-state [22].

3.3. Magnetic properties

Saturation magnetization measurements show a decrease with increased milling time (Fig. 8). Previous studies have noted change in saturation with increased milling time [20,21,23,27]. They have attributed this to increased contamination with milling time [17]. Common contaminants are from the steel media used during milling, Fe, Cr, and potentially oxygen [20,23]. The saturation magnetization is also shown to decrease with increasing Si content (Fig. 9) which is consistent with diamagnetic Si ions neighboring Fe ones, thus reducing the overall magnetic moment [28].

The coercivity before milling is low because of the large grain-size in the initial Fe particles, and it increases after milling and remains at a near constant value with increased milling time. Coercivity, in general is affected by defects such as dislocations, grain boundaries, inclusions and voids. In polycrystalline materials, the coercivity is also affected by grain size because of the interaction of domain walls with grain boundaries. As grain size decreases, the larger volume fraction of grain boundaries causes an increase in coercivity due to boundaries impeding domain wall (Bloch wall) motion. However, the coercivity is greatly reduced as grain size decreases further. As the grain size approaches the ferromagnetic correlation length (20–40 nm for iron-based alloys [12]), randomly-oriented neighboring grains produce an averaging effect on the magnetocrystalline anisotropy, effectively lowering it [12,13,29]. This means that the nanodomains offer less resistance to Bloch walls and coercivity approaches very low values [13]. Based on the random anisotropy model, the coercivity can be expressed as [30]:

$$H_c = \frac{p_c k_1^4 D^6}{\mu_0 M_s A^3}$$

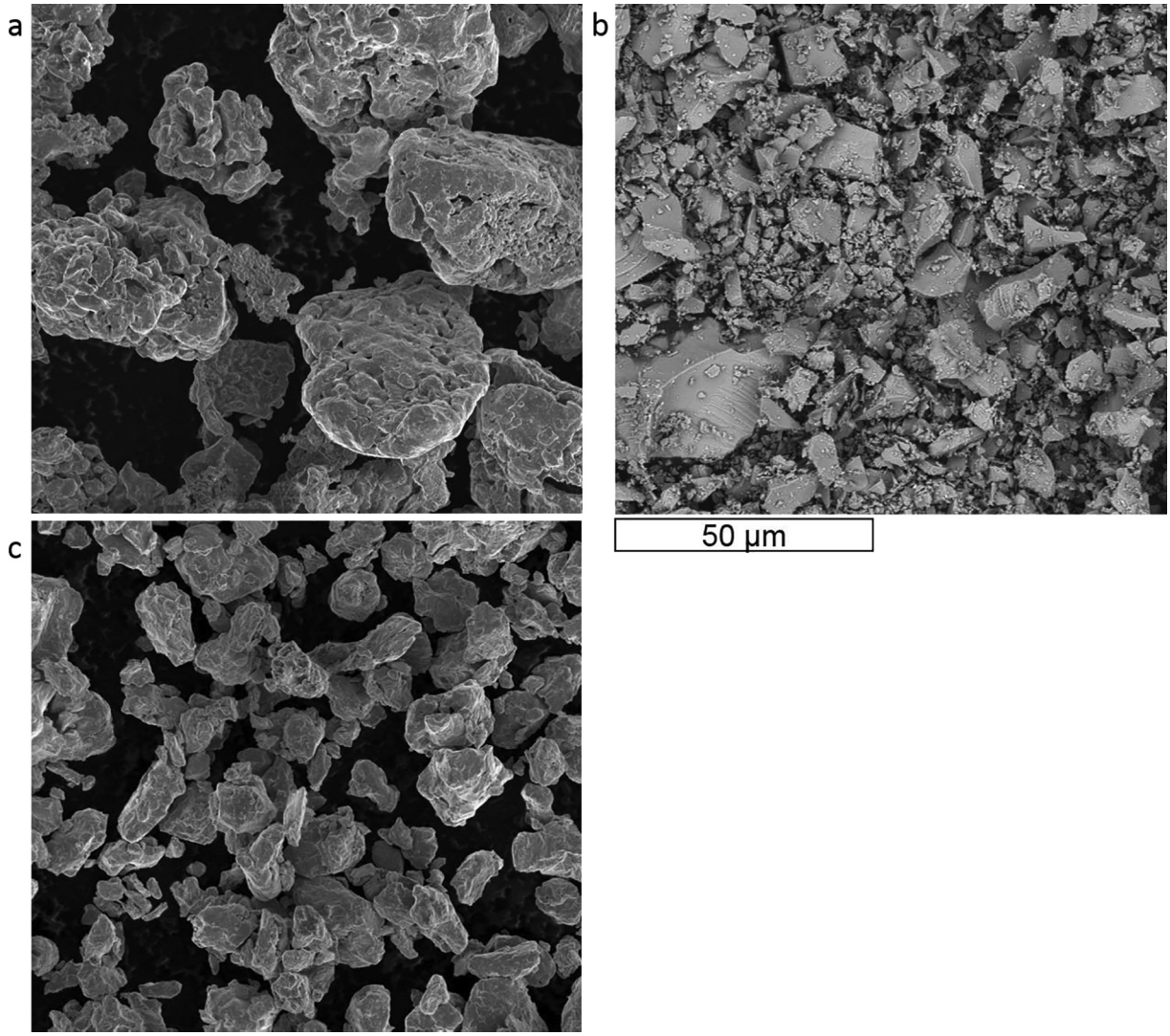

Fig. 1. SEM micrographs of (a) as-received Fe, (b) Si, and (c) mechanically alloyed FeSi 3.5 wt%.

where p_c is a constant of order unity, and μ_0 is the permeability of free space. Other studies have observed disagreement with the coercivity values predicted by the random anisotropy model [20,23,27]. They have attributed this difference to high degrees of strain remaining in the lattice [27], which after annealing brings the coercivity more in line with that predicted by this model [20,31].

The coercivity values as a function of Si content are all similar (Fig. 9), and are larger than the values on the order of 0.1–1 Oe predicted by the random anisotropy model [12]. In addition to the lattice strain previously described, underestimation of the grain size and uniformity can also impact the coercivity. As described by Li et al., grain size, grain size distribution as well as grain boundary chemistry can affect coercivity [27]. If grain size is underestimated by x-ray diffraction, then there will be an observed lesser effect on coercivity than expected. X-ray analysis also provides an estimated average grain size where there can be a distribution of grain sizes. The grains larger than 20–40 nm will not contribute to reducing magnetocrystalline anisotropy and thus there will be a reduced effect on minimizing coercivity.

There may also be some contribution of grain boundary characteristics to the increased coercivity that are not being accounted for by this model, for example, segregation of the solutes to boundaries that may inhibit magnetic coupling between neighboring grains. The degree of exchange interaction between grains depends on the thickness and magnetic structure of their interface at the grain boundary, with narrow grain boundaries resulting in a highly-coupled exchange interaction between neighboring grains [12]. If the grain boundaries are occupied by a nonmagnetic or less magnetic elements such as Si, it is possible to reduce the effects of the exchange interaction and random anisotropy.

4. Conclusion

Mechanical alloying of elemental Fe and Si powders resulted in a disordered BCC solid solution as indicated by XRD measurements. Increased milling time reduces the particle size, and the particle size distribution becomes narrower. Grain size decreases to about 15 nm after 5 h of milling and remains constant with increased milling times. Increased milling time also reduces the saturation magnetization. This is due to contaminants being introduced from the stainless-steel media.

Increased Si content above the equilibrium saturation concentration does not result in any formation of detrimental D03 ordered phase. The grain size is constant with increasing Si content after 5 h of milling. The small change in Si concentration examined does not affect the minimum grain size. The magnetic saturation decreases with increasing Si due to its diamagnetic nature lowering the average atomic magnetization.

Coercivity measurements are higher than predicted from the random anisotropy model and measured grain size due to high lattice strain and imprecision of grain size calculation using x-ray analysis.

This work shows that soft magnetic powders can be mechanically

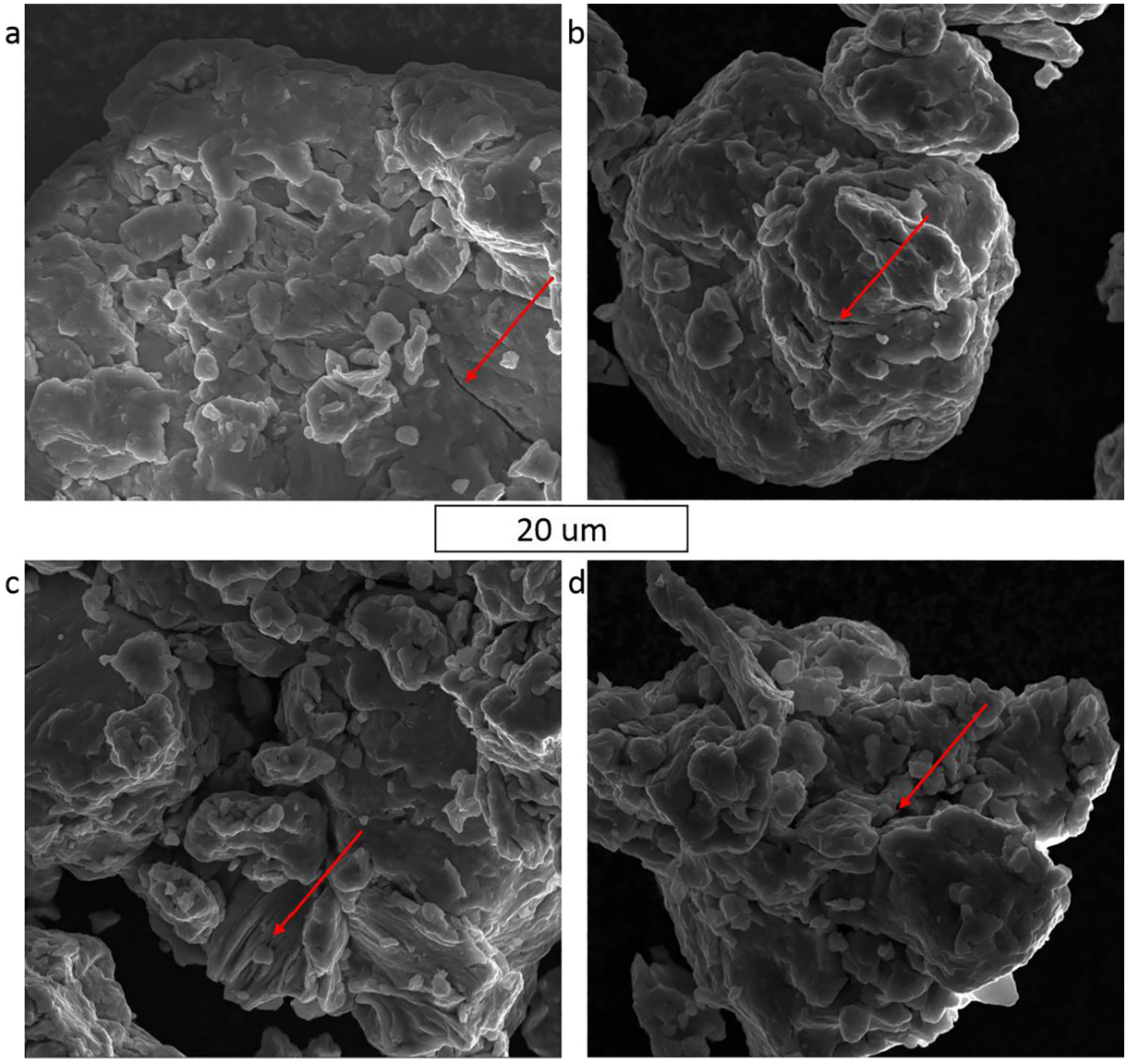

Fig. 2. SEM micrographs of lamellar structure and agglomerated particles of FeSi 3.5 wt% milled for (a) 5 h, (b) 10 h, (c) 15 h, and (d) 20 h. The arrows in the figure indicate large particle fracture sites (a, b, d) and lamella (c).

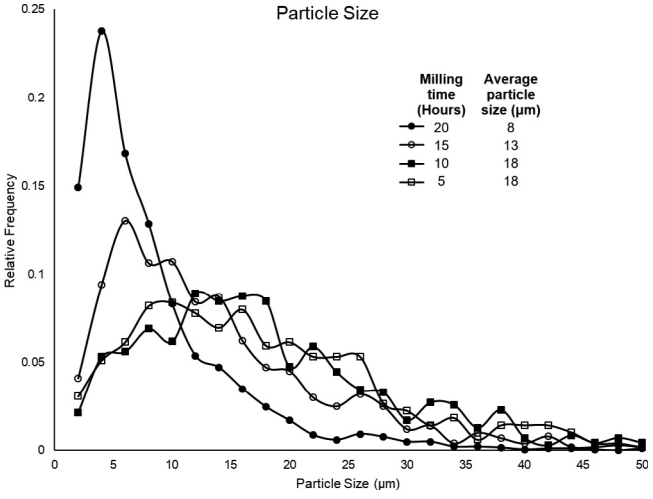

Fig. 3. Particle size distribution of mechanically alloyed Fe 3.5 wt% Si milled for 5, 10, 15, and 20 h.

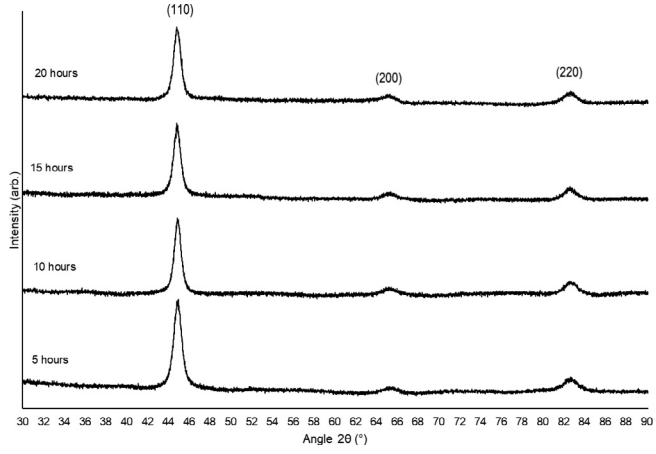

Fig. 4. X-ray diffraction spectra of mechanically alloyed Fe 3.5 wt% Si milled for 5, 10, 15, and 20 h.

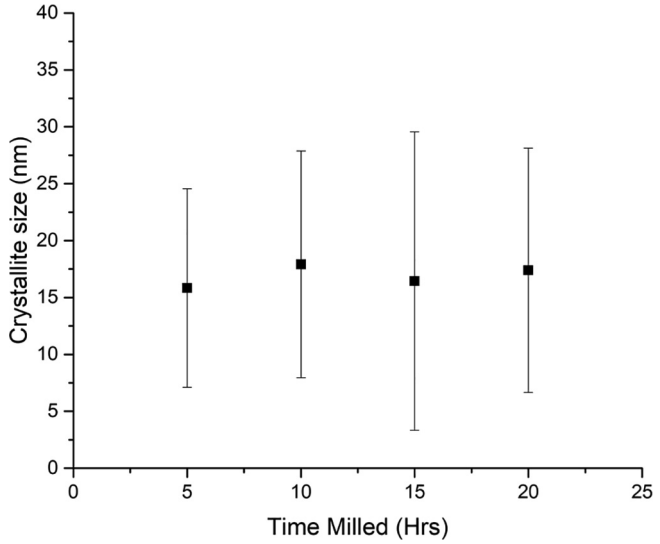

Fig. 5. Crystallite size of Fe 3.5 wt% Si after 5, 10, 15, 20 h of milling.

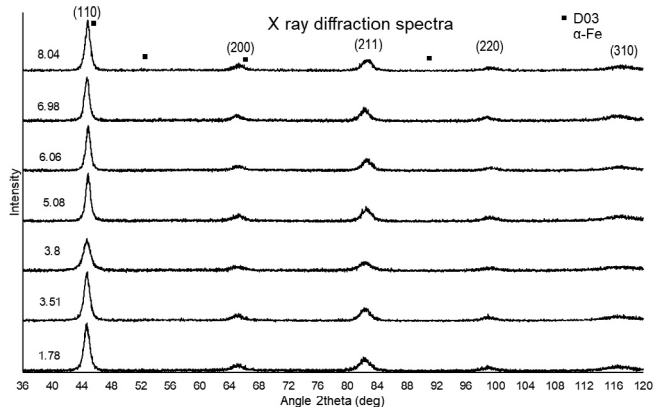

Fig. 6. X-ray diffraction spectra of FeSi alloys with Si wt% 1.78, 3.51, 3.8, 5.08, 6.06, 6.98, 8.04.

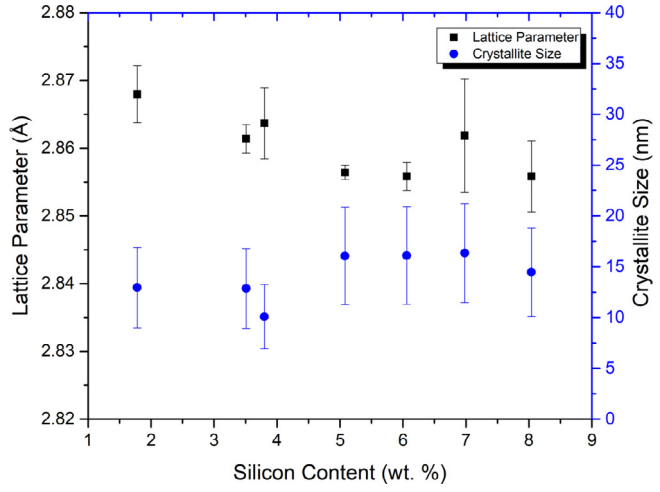

Fig. 7. Unit cell parameter (squares) and average crystallite size (circles) of mechanically alloyed FeSi alloys.

alloyed with refined nanocrystalline microstructure in much faster times than previously reported via the use of high-energy mixing approaches. These findings lead us to hypothesize that higher energy ball milling can lead to similar microstructure and magnetic properties to those reported by lower energy processes after longer processing times.

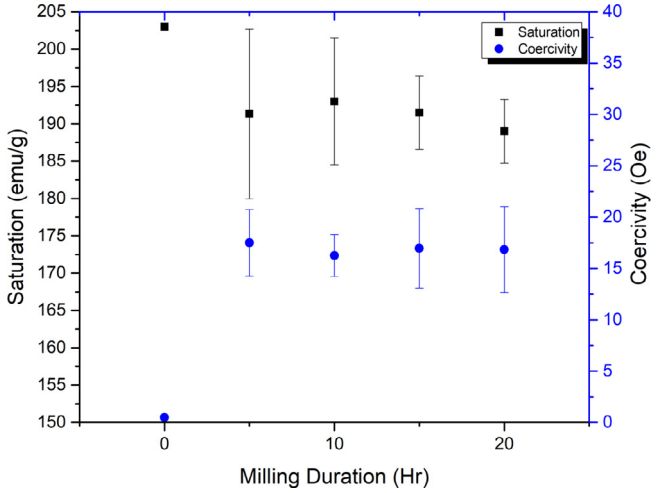

Fig. 8. Magnetic saturation and coercivity of Fe 3.5 wt% Si with milling times 0, 5, 10, 15, 20 h.

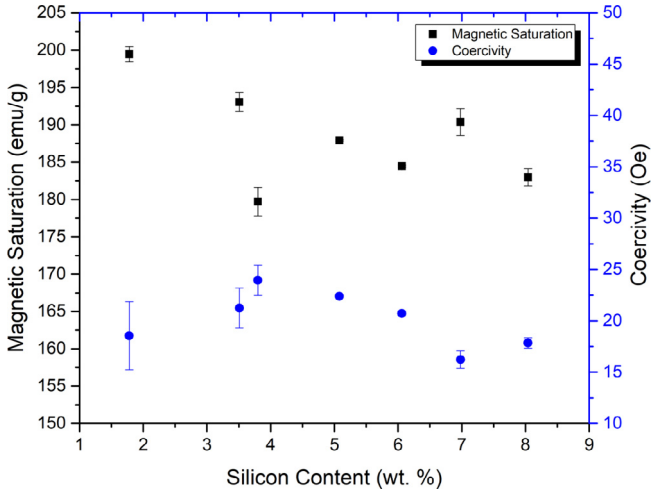

Fig. 9. Magnetic saturation and coercivity of mechanically alloyed FeSi alloys.

The processing-structure-properties relationships discussed here will be useful for further research into nanocrystalline soft magnetic materials in applications such as electric motors, inductors, and transformer cores.

Acknowledgements

This research was supported by the MS^3 (Materials Synthesis and Simulation across Scales) initiative at Pacific Northwest National Laboratory (PNNL), a multi-program national laboratory operated by Battelle for the U.S. Department of Energy (DOE). Microscopy was carried out in the Center for Advanced Microscopy and Microanalysis (CFAMM) at the University of California, Riverside.

References

[1] S. Chikazumi, C.D. Graham, Physics of Ferromagnetism, Oxford University Press, 1997.
[2] S. Arajs, H. Chessin, D.S. Miller, First magnetocrystalline anisotropy constants of some iron-silicon alloys, J. Appl. Phys. 32 (5) (May 1961) 857–859.
[3] R.M. Bozarth, Ferromagnetism, first ed., Van Nostrand, Amsterdam, 1951.
[4] W.J. Carr, R. Smoluchowski, The magnetostriction of single crystals of iron-silicon alloys, Phys. Rev. 83 (6) (1951) 1236–1243.
[5] K.I. Arai, Y.H. Kim, M. Yamaguchi, K. Ishiyama, Eddy-current losses and number of domain-walls with respect to total number of layers for very thin 3-percent Si-Fe strip-wound cores, J. Magn. Magn. Mater. 133 (1–3) (1994) 198–200.
[6] P.R. Swann, L. Grånäs, B. Lehtinen, The B2 and DO3 ordering reactions in iron-

silicon alloys in the vicinity of the curie temperature, Met. Sci. 9 (1) (1975) 90–96.
[7] Y. Zhang, D.G. Ivey, Fe3Si formation in Fe-Si diffusion couples, J. Mater. Sci. 33 (12) (1998) 3131–3135.
[8] D. Bouchara, M. Fagot, J. Degauque, J. Bras, Ordering influence on magnetic properties of rapidly quenched Fe-6.5 wt% Si, J. Magn. Magn. Mater. 83 (1–3) (1990) 377–378.
[9] M.E. McHenry, M.A. Willard, D.E. Laughlin, Amorphous and nanocrystalline materials for applications as soft magnets, Prog. Mater. Sci. 44 (4) (1999).
[10] Wei Shen, Fei Wang, D. Boroyevich, C.W. Tipton, Loss characterization and calculation of nanocrystalline cores for high-frequency magnetics applications, IEEE Trans. Power Electron. 23 (1) (2008) 475–484.
[11] M.A. Meyers, A. Mishra, D.J. Benson, Mechanical properties of nanocrystalline materials, Prog. Mater. Sci. 51 (4) (2006) 427–556.
[12] G. Herzer, Modern soft magnets: amorphous and nanocrystalline materials, Acta Mater. 61 (3) (2013) 718–734.
[13] G. Herzer, Grain size dependence of coercivity and permeability in nanocrystalline ferromagnets, IEEE Trans. Magn. 26 (5) (1990) 1397–1402.
[14] L. Takacs, J.S. McHenry, Temperature of the milling balls in shaker and planetary mills, J. Mater. Sci. 41 (2006) 5246–5249.
[15] C. Suryanarayana, Mechanical alloying and milling, Prog. Mater. Sci. 46 (1–2) (Jan. 2001) 1–184.
[16] O. Kohmoto, N. Yamaguchi, T. Mori, Preparation of 6.5 wt% Si-Fe by mechanical alloying, J. Mater. Sci. 29 (12) (1994) 3221–3223.
[17] R.J. Perez, B.-L. Huang, P.J. Crawford, A.A. Sharif, E.J. Lavernia, Synthesis of nanocrystalline Fe-B-Si powders, Nanostruct. Mater. 7 (1–2) (Jan. 1996) 47–56.
[18] A. Zolriasatein, A. Shokuhfar, F. Safari, N. Abdi, Comparative study of SPEX and planetary milling methods for the fabrication of complex metallic alloy nanoparticles, Micro Nano Lett. 13 (2017) 448–451.
[19] C.C. Koch, O.B. Cavin, C.G. McKamey, J.O. Scarbrough, Preparation of "'amorphous"' $Ni_{60}Nb_{40}$ by mechanical alloying, Appl. Phys. Lett. 43 (11) (1983) 1017–1019.
[20] J. Ding, et al., Microstructure and soft magnetic properties of nanocrystalline Fe-Si powders, J. Alloys Compd. 314 (1–2) (2001) 262–267.
[21] M. Abdellaoui, T. Barradi, E. Gaffet, Mechanism of mechanical alloying phase formation and related magnetic and mechanical properties in the FeSi system, J. Alloys Compd. 198 (1–2) (1993) 155–164.
[22] A.H. Bahrami, S. Sharafi, H. Ahmadian Baghbaderani, The effect of Si addition on the microstructure and magnetic properties of permalloy prepared by mechanical alloying method, Adv. Powder Technol. 24 (1) (2013) 235–241.
[23] C.D. Stanciu, T.F. Marinca, I. Chicinaş, O. Isnard, Characterisation of the Fe-10 wt% Si nanocrystalline powder obtained by mechanical alloying and annealing, J. Magn. Magn. Mater. 441 (2017) 455–464.
[24] S. Miraghaei, P. Abachi, H.R. Madaah-Hosseini, A. Bahrami, Characterization of mechanically alloyed Fe100-xSix and Fe83.5Si13.5Nb3 nanocrystalline powders, J. Mater. Process. Technol. 203 (1–3) (2008) 554–560.
[25] M. Khajepour, S. Sharafi, Structural and magnetic properties of nanostructured Fe50(Co50)–6.5 wt% Si powder prepared by high energy ball milling, J. Alloys Compd. 509 (29) (2011) 7729–7737.
[26] M.L. Öveçoglu, C. Suryanarayana, W.D. Nix, Identification of precipitate phases in a mechanically alloyed rapidly solidified Al-Fe-Ce alloy, Metall. Mater. Trans. A 27 (4) (1996) 1033–1041.
[27] M. Li, R. Birringer, W.L. Johnson, R.D. Shull, Nanocrystalline Fe-Si phase by mechanical attrition and its soft magnetic properties, Nanostruct. Mater. 3 (1993) 407–412.
[28] N.R. Overman, et al., Physical and electrical properties of melt-spun Fe-Si (3–8 wt %) soft magnetic ribbons, Mater. Charact. 136 (2017) 212–220 2018.
[29] M.E. McHenry, D.E. Laughlin, Nano-scale materials development for future magnetic applications, Acta Mater. 48 (1) (2000) 223–238.
[30] W. Wernsdorfer, K. Suzuki, G. Herzer, Mol. Nanomagnet. (2006).
[31] M.A. Cunha, G.W. Johnson, Rapidly solidified Si-Fe alloys, J. Mater. Sci. 25 (5) (1990) 2481–2486.